Available online at www.sciencedirect.com
SCIENCE DIRECT®
Journal of Chromatography A, 1033 (2004) 71–82
JOURNAL OF CHROMATOGRAPHY A
www.elsevier.com/locate/chroma

Methodologies for model calibration to assist the design of a preparative ion-exchange step for antibody purification

David Karlsson [a], Niklas Jakobsson [a], Karl-Johan Brink [b], Anders Axelsson [a], Bernt Nilsson [a,*]

[a] *Department of Chemical Engineering, Center for Chemistry and Chemical Engineering, P.O. Box 124, SE-221 00 Lund, Sweden*
[b] *BioInvent International AB, SE-223 70 Lund, Sweden*

Received 16 October 2003; accepted 24 December 2003

Abstract

This work proposes methodologies using a model-based approach to gain knowledge on and assist the development of an ion-exchange step in a protein purification process; the separation of IgG from a mixture containing IgG, insulin and transferrin. This approach is suitable for capture and intermediate steps in a process. Both methods involve four consecutive steps. Firstly, the retention of the different protein components is determined giving a retention map of the system. From this the optimal pH and buffer can be determined. Secondly, additional salt gradient experiments are performed at the selected pH. Thirdly, experimental breakthrough curves have to be generated for the protein if the adsorption capacity of the medium for each component is not known. Fourthly, a validation experiment is performed. In method 1, where the capacity for the medium is assumed to be known, the protein adsorption is described by Langmuir kinetics with a mobile phase modulator (MPM). In this description salt is considered to be inert. In method 2 the adsorption behavior is described by steric mass action (SMA), where the salt component competes with the proteins for the available binding sites. Both methods use a dispersion model to describe transport in the mobile phase in the column. The methods are able to predict the separation and loading behavior of the three components. The methods can, with reasonable accuracy, predict the breakthrough of transferrin in a mixture of insulin, IgG and transferrin. Method 1 requires fewer experiments and predicts the mean volume of breakthrough for the loading step in the validation experiment more accurately than method 2. On the other hand, method 2 has a better accuracy to predict the position of 10% breakthrough and the shape of the breakthrough curve. The methods suggested in this work are shown to be efficient in process development. Some additional experiments have to be performed to obtain the unknown parameters in the models. However, the predictability that is achieved results in less experimental work in the process design as a whole.

Keywords: Model calibration; Antibody purification; Dynamic simulation; Downstream processing; Steric mass action; Mobile phase modulator; Langmuir kinetics

1. Introduction

Today, design and optimization are becoming extremely important in bioseparation as the process of development of a biotech product is becoming more and more expensive [1]. It is believed that it will be possible to reduce the number of labor-intensive experiments, and thereby shorten the time and reduce the cost, by modeling and simulation in the design and optimization of a process. This requires a methodology employing accurate models validated by carefully designed experiments when developing a new separation step in the downstream process. The employed models should preferably be based on an understanding of the underlying physical mechanisms.

One type of protein to which much attention is being given in the biopharmaceutical industry is antibodies [2]. The antibody or the antibody fragments can be expressed in plants [3], animals [4], bacteria [5] or, most important of all, in a mammalian cell culture [6]. The high cost incurred by the antibody-producing companies is, however, due to the downstream processing, constituting 80% of the total cost [7]. Consequently, a cheap method of designing and optimizing a purification step well is required.

* Corresponding author. Tel.: +46-46-2228088; fax: +46-46-2224526.
E-mail address: bernt.nilsson@chemeng.lth.se (B. Nilsson).

0021-9673/$ – see front matter © 2004 Elsevier B.V. All rights reserved.
doi:10.1016/j.chroma.2003.12.072

Many techniques are available to purify antibodies, such as ion-exchange chromatography (IEC) [8], affinity chromatography [9], hydrophobic interaction chromatography (HIC) [10], gel filtration [11], membrane separation [12] and precipitation [13]. Today, chromatography is the most common technique in commercial processes. This work focuses on ion-exchange chromatography.

The principle of ion-exchange chromatography is that species with a net charge opposite to the ligands interact with the charged groups on the stationary phase used in chromatography and pass through the column slowly or not at all. Species with no net charge or the same charge as the ligands on the matrix will pass completely through the column. The net charge depends on the amino acid sequence, the pK_a of the ionic groups and the pH of the solution [14]. The isoelectric point (pI), i.e. the pH at which the net charge on the protein is zero, varies from 4 to 9 for antibodies, most of them having a pI over 6, which is often more basic than serum proteins which are common in fermentation [15]. Antibodies are usually stable over a wide pH range, which makes IEC useful as a purification technique. One practical limitation is that the feed to the column must be of a relatively low ionic strength, which often leads to the requirement of preceding dilution of the fermentation broth or buffer change by diafiltration.

The best conditions for separation are often determined from a retention map [16]. This is obtained by a series of rapid separations for both cation- and anion-exchangers, using the same salt gradient, but over a range of pH. The elution volume is plotted against pH for each elution peak. An analysis of the plot regarding the point of maximum separation between the product and the other components will indicate at what pH and with which IEC medium maximum resolution is expected. The selected pH gives the most suitable buffer. This approach has been used in this work.

This work proposes two different methods using a model-based approach to gain knowledge on and assist in the development of an ion-exchange step in a protein purification process. This approach is suitable in capture, the first purification step after the expression system, and in the intermediate steps, following after the capture. The methods studied here require just a few additional experiments besides those required for the retention map and a validation experiment.

2. Theory—models and simulation techniques

The two methodologies utilize different mathematical models for the chromatography step. In the first model the protein adsorption is described by Langmuir kinetics with a mobile phase modulator (MPM) [17]. In this description salt is considered to be inert. The second model uses a steric mass action adsorption model (SMA) [18] where the salt component competes with the proteins for the available binding sites. Both models use a dispersion model to describe the transport in the mobile phase in the column [19].

2.1. Column model

A column described by a kinetic/dispersion model contains one part describing the dispersion and convection in the mobile phase, and another part describing the adsorption. In the models used in this work the shapes of an elution peak and breakthrough curve are dependant on an apparent dispersion coefficient and of the adsorption rate. The column model for component i is described by the following equation, see Eq. (1):

$$\frac{\mathrm{d}c_i}{\mathrm{d}t} = D_{\mathrm{ax}}\frac{\partial^2 c_i}{\partial x^2} - v_{\mathrm{int}}\frac{\partial c_i}{\partial x} - \frac{1-\varepsilon_{\mathrm{c}}}{\varepsilon_{\mathrm{c}}}\frac{\mathrm{d}q_i}{\mathrm{d}t} \tag{1}$$

where ε_{c} is the void fraction in the packed bed (m^3 mobile phase/m^3 column), x the axial coordinate along the column (m), v_{int} the interstitial velocity (m/s), D_{ax} the apparent dispersion coefficient (m^2/s), c_i the concentration of component i in the mobile phase (mol/m^3), q_i the concentration of component i in the stationary phase (mol/m^3 gel) and t is the time (s).

The column equation is subject to the following boundary conditions.

A Robin condition describes the column inlet, Eq. (2).

$$\frac{\partial c_i}{\partial x} = \frac{v_{\mathrm{int}}}{D_{\mathrm{ax}}}(c_i - c_{\mathrm{inlet},i}) \quad \text{at } x = 0 \tag{2}$$

where $c_{\mathrm{inlet},i}$ is the inlet concentration (mol/m^3) and c_i is the concentration just inside the column (mol/m^3), which may be slightly lower than $c_{\mathrm{inlet},i}$ due to the dispersion at the inlet. At the outlet where x is equal to L, the length of the column (m), only convective transport is considered and can thus be described by a Neumann condition, see Eq. (3).

$$\frac{\partial c_i}{\partial x} = 0 \quad \text{at } x = L \tag{3}$$

Both models include competition for the available binding sites. The studied protein mixture contains proteins of various sizes with uniformly distributed and equi-accessible fixed charges at the surface as binding sites. Proteins of different sizes have different access to the binding sites on the gel because large proteins are not able to penetrate into the smaller pores.

The differences in protein size give rise to different binding conditions in different parts of the gel. In the parts where all three proteins can compete for binding sites the binding conditions will be competitive. The smallest protein will be able to access parts of the gel that no other protein can reach and thus bind without competing proteins in this region. Using this model implies that the effects of different porosity for the proteins are not accounted for.

2.2. Adsorption—Langmuir MPM model

In this description the adsorption is described by Langmuir kinetics [19], see Eq. (4). The adsorption and desorption of the protein are regarded as competitive processes where the salt concentration effects the retention of the protein. Because salt is considered to be inert, dq_{salt}/dt is zero. During the binding step, $k_{ads,i}$, the adsorption coefficient of component i (m^3/mol s), is much larger than $k_{des,i}$, the desorption coefficient of component i (1/s), while at elution $k_{des,i}$ dominates.

$$\frac{dq_i}{dt} = k_{ads,i}c_i(q_{max,i} - q_i) - k_{des,i}q_i \quad (4)$$

$q_{max,i}$ is the maximum concentration of component i in the stationary phase (mol/m^3 gel).

The model can be used for the loading step as well as the elution step by using mobile phase modulators [20], defined by Eqs. (5) and (6):

$$k_{ads,i} = k_{ads0,i}e^{\gamma_i S} \quad (5)$$

$$k_{des,i} = k_{des0,i}S^{\beta_i} \quad (6)$$

where S is the concentration of the elution component, often salt, and $k_{ads0,i}$ (m^3/mol s) and $k_{des0,i}$ (m^3/mol s) are constants. β_i is a constant describing the ion-exchange characteristic and γ_i (m^3/mol) describes the HIC characteristic. Under loading conditions, S is given by the buffer salt concentration only, i.e. $k_{ads,i} \approx k_{ads0,i}$ and $k_{des,i} \approx 0$ unlike the elution conditions ($S > 0$), where S is reduced by the factor $e^{\gamma S}$ and $k_{des,i}$ is increased by a factor $S^{\beta i}$. The assumption that hydrophobic interactions are absent is made in this work, which means that γ_i is equal to zero. Although hydrophobic interactions are neglected the effect of these could be seen from a parameter study of the model by tuning the γ_i factor.

2.3. Adsorption—the Steric Mass Action model

In the second method the adsorption is described by steric mass action [18]. The interaction between protein and the solid phase in the SMA model is described as an equilibrium reaction where electro-neutrality must be conserved. Protein and salt compete for the available binding sites on the gel, and salt is no longer treated as an inert component in this model. When protein binds to the gel, the binding sites on the protein occupy a number of ligands. The bound protein also shields a number of ligands due to its size [18].

The interaction between a number of salt ions and a protein molecule is modeled as an equilibrium reaction between protein in the mobile phase, c_i, and available salt ions, $\bar{q}_s$, in the gel, see Eq. (7).

$$c_i + \nu_i\bar{q}_s \underset{k^*_{des}}{\overset{k^*_{ads}}{\leftrightarrow}} q_i + \nu_i c_s \quad (7)$$

where c_i is the concentration in the mobile phase and q_i the concentration in the stationary phase. $\bar{q}_s$ is the concentration of available sites in the gel and ν is the number of interacting sites between protein and gel. $k^*_{ads,i}$ and $k^*_{des,i}$ are the rate constants for adsorption and desorption, respectively; s and i denote salt and protein, respectively.

At equilibrium, Eq. (8) is obtained:

$$\frac{k^*_{des,i}}{k^*_{ads,i}} = K_{eq,i} = \left(\frac{c_i}{q_i}\right)\left(\frac{\bar{q}_s}{c_s}\right)^{\nu_i} \quad (8)$$

The concentration of unavailable salt ions, due to steric hindrance by bound protein molecules, is given by Eq. (9):

$$\hat{q}_s = \sum_{i=1}^{N}\sigma_i q_i \quad (9)$$

Here $\hat{q}_s$ is the concentration of shielded ligands in the gel and N is the number of interacting components. The steric factor, σ_i, describes the number of shielded ligands per bound protein molecule.

The total concentration of salt in the gel is given by the sum of available and unavailable sites, as in Eq. (10):

$$q_s = \bar{q}_s + \hat{q}_s \quad (10)$$

The total concentration of sites in the gel can also be described by Eq. (11):

$$\Lambda = \bar{q}_s + \sum_{i=1}^{N}(\nu_i + \sigma_i)q_i \quad (11)$$

The adsorption/desorption reaction, r, can be described by Eq. (12):

$$r_i = k^*_{ads,i}c_i\bar{q}_s^{\nu_i} - k^*_{des,i}q_i c_s^{\nu_i} \quad (12)$$

The ratio between $k^*_{ads,i}$ and $k^*_{des,i}$ is set by the equilibrium association constant, $K_{eq,i}$. The result is that the interaction is modeled as a reaction at equilibrium with some adsorption kinetics. The change in protein concentration in the gel is equal to the adsorption kinetic, see Eq. (13).

$$\frac{dq_i}{dt} = r_i \quad (13)$$

The change in concentration of ligands in the gel is determined by the conservation of electro-neutrality, see Eq. (14).

$$\frac{dq_s}{dt} = -\sum_{i=1}^{N}\nu_i\frac{dq_i}{dt} \quad (14)$$

The number of available ligands is given by combining Eqs. (9) and (10), see Eq. (15).

$$\bar{q}_s = q_s - \sum_{i=1}^{N}\sigma_i q_i \quad (15)$$

2.4. Simulation techniques

Using the method of lines (MOL), each partial differential equation in the Langmuir MPM model is discretized in

space, three-point finite difference, to give a set of ordinary differential equations. The space is divided into a set of grid points, where each grid point contains a discretized ordinary differential equation. For this model the number of grid points was set to 60, which is enough to avoid numerical dispersion. This was solved with a standard solver for ordinary differential equations (ODE15S) in MATLAB [21].

The SMA model is implemented using a modeling and simulation tool called gPROMS developed by Process System Enterprise [22]. The column model is simulated using a finite difference approximation and a fourth order approximation for the linear solver of the resulting set of differential equations. The number of grid points in the column is set to 400 to ensure that there is no numerical broadening in the column. The apparent dispersion coefficient and the kinetics of the solid phase interaction describe the peak broadening effect.

3. General approach

The approach suggested in this work can be seen as a protocol for model calibration to assist the development of an ion-exchange step. Methods 1 and 2 involve four consecutive steps, partly experimental end partly performed by simulation, described in the following section. The methods differ in step three. Each step involves a certain kind of experiment and a decision or an estimation of some parameters in the models. The first method utilizing the Langmuir MPM model requires fewer experiments than the second method utilizing the SMA model.

1. Retention map

   Eleven experiments are performed on the clarified fermentation broth from pH 3.5 to 8.5 with the same salt concentration, salt gradient and flow. The main goal is to achieve optimal resolution.

Decision
Optimal pH Suitable buffer

   If screening for different media and columns is required a decision on column and medium is also made. This will give several retention maps, and was not the focus in this work.
2. Additional gradients

   Three additional salt gradient experiments are performed in order to estimate the linear parameters in both models. The kinetic parameter k_{des0} is adjusted to give a reasonable peak width.

Output
Method 1: $k_{ads0,i}$, $k_{des0,i}$ and β_i Method 2: $K_{eq,i}$ and ν_i

Table 1
The number of experiments, number of parameters in the model and the number of fitted parameters for each model-based method

	Model	Number of experiments	Number of parameters in the model	Number of fitted parameters
Method 1	Langmuir MPM model	15	6	6
Method 2	SMA model	18	6	15

3. Pure component experiments/empirical correlations

   Method 1 uses data from the column medium supplier to estimate the adsorption capacity of the medium for each component and uses an empirical equation and the gradient elution experiments to describe the peak broadening effect in the column. This is necessary if the pure components are not available.

   To obtain the adsorption capacity of the medium in method 2, experiments with breakthrough curves for each component is performed. This gives the non-linear equilibrium parameter, σ_i, and the shape parameters in the SMA model.

Output
Method 1: $q_{max,i}$ and D_{ax} Method 2: σ_i, D_{ax} and $k_{des,i}$

4. Validation experiment

   To ascertain that the models are correct, a final validation experiment is performed on a clarified fermentation broth with salt content and protein concentrations not used in the previous parameter estimation.

   The number of experiments and parameters for the two methods are presented in Table 1.

3.1. Method 1

Method 1 requires only two additional gradient experiments besides the retention maps often used in the development of an ion-exchange purification step. The number of experiments will not change when new components are included. The shape and capacity parameters are taken from the column medium supplier, from empirical correlations and from the gradient elution experiments.

The number of fitted parameters will increase by two for each new component included.

3.2. Method 2

Method 2 requires an additional single component experiment to obtain the capacity and shape parameters for each component. The number of experiments will increase by one for each new component included. The number of fitted parameters will increase by five for each new component included.

4. Materials and methods

4.1. Materials

The columns used in the chromatography experiments were RESOURCE 15 Q and 15 S, 1 ml (No. 920408) pre-packed columns (diameter 6.4 mm, length 30 mm supplied by Amersham Biosciences, Uppsala, Sweden).

Chromatography experiments were carried out on two different chromatography systems. Gradient elution experiments were performed on a ÄKTA explorer 100 system from Amersham Bioscience (Uppsala, Sweden) and breakthrough experiments were carried out on a ÄKTA purifier 100 system from Amersham Bioscience (Uppsala, Sweden). The gradient elution experiments were performed in cooperation with BioInvent International AB (Lund, Sweden). The gradient elution experiments were conducted on a fermentation broth from serum-free media containing three major components, namely IgG, transferrin and insulin.

The breakthrough experiments were carried out on pure components: insulin (I-5500, Lot No. 30K1310) (Bovine Pancreas, EC No. 234-291-2) and holo-transferrin (T-4132, Lot No. 121K7611) (Siderophilin, iron-saturated, EC No. 234-318-8), both obtained from Sigma.

Trizma base was also obtained from Sigma. NaCl was obtained from Merck (Darmstadt, Germany). Buffers used for the breakthrough experiments were 0.1 M Tris–HCl buffers at pH 8.5 and 0.1 M Tris–HCl at pH 8.5 with 1 M NaCl.

4.2. Methods

4.2.1. Gradient experiments to determine the linear parameters in the models

The parameters ν_i and $K_{eq,i}$ in the SMA model and the parameters $k_{ads0,i}/k_{des0,i}$ and β_i in the Langmuir MPM model can be found by running gradient elution experiments with different gradients [23].

To find the optimal pH for the gradient elution, a retention map was established for the fermentation broth, see Fig. 1. pH 8.5 was considered most promising and gradient elution was performed with different gradients. The linear gradients at pH 8.5 used for parameter estimation were 40, 60, 80 and 160 column volumes (CV). The results were compensated for dead volumes in the system to isolate the behavior due to the column. The parameters were fitted by computer simulation to match the peak position for the different pH values. The computer simulation includes the loading time, loading concentration of the different proteins, column wash, conductivity in the loading sample and length of gradient.

The fermentation broth has a high concentration of IgG and the IgG peak partly conceals the other peaks. IgG was partly removed from the sample with affinity chromatography and the loading sample was spiked with insulin and transferrin to give differentiable peaks in the chromatogram. The inlet concentrations were diluted online 10 times to 0.02 mg/ml IgG, 0.06 mg/ml insulin and 0.03 mg/ml transferrin. The fermentation broth has a conductivity of 15 mS/cm and was diluted to about 1 mS/cm at pH 8.5. The final conductivity at the end of the elution was 84 mS/cm. The elution buffer was 0.1 M Tris–HCl pH 8.5 with 1 M NaCl. The flow rate for all gradient elution experiments was 4 ml/min. The loading step lasted 46 column volumes and the column was washed with two column volumes of buffer.

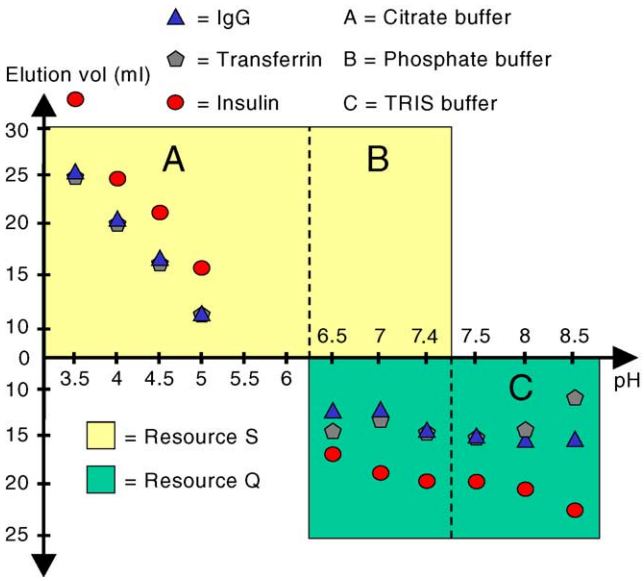

Fig. 1. The retention map that describes elution volume when the different proteins are eluted at various pH values.

4.2.2. Experiments to determine the steric factor and the kinetics in the SMA model

The steric factor can be determined by breakthrough experiments for each pure component at a high protein concentration [24]. In the original SMA estimation technique the steric factor was calculated algebraically from $q_{max,i}$ by performing a breakthrough experiment at high protein concentration [25].

In this study, the breakthrough experiments had to be performed at sufficiently high protein concentration to lie in the non-linear part of the isotherm. The ideal experiment is of course continued to 100% breakthrough but this requires large amounts of protein. However, when the breakthrough experiments are performed the isotherm is not known. It is thus difficult to estimate a suitable protein concentration for the experiment. In general, it can be stated that a protein concentration at which the position of the breakthrough curve is clearly dependent on the steric factor is high enough. The steric factor is altered in the simulation to give the correct amount of bound protein.

The breakthrough experiments were conducted at pH 8.5 and the conductivity of the sample was approximately 3 mS/cm. The conductivity of the elution buffer (Tris–HCl buffer, 1 M NaCl) was approximately 82 mS/cm. The breakthrough experiments were carried out at different protein concentrations to validate the steric factor for each pro-

tein. The flow rate was maintained at 1 ml/min in each run. Insulin has a very low solubility around neutral pH and special measures had to be taken when preparing the insulin samples. Insulin was mixed with Tris–HCl buffer at pH 8.5 and the pH was raised with dilute NaOH until the solution became clear. The pH was then adjusted by dilute HCl to restore the pH to 8.5. The result of this treatment is a higher conductivity in the insulin experiments, which has to be considered in the parameter estimation.

4.2.3. Experiments to determine the dead volume in the chromatography systems

The ÄKTA Purifier system has a relatively low dead volume for the sample when using a superloop in the injection of the sample. The dead volume in the ÄKTA Purifier system was found to be 0.18 ml in the experimental set-up used.

The ÄKTA Explorer system is a more advanced chromatography system with a larger dead volume. The system used has a dead volume between the column and the UV detector of 2 ml, and the dead volume associated with the conductivity cell upstream of the column is 1.7 ml. The peak position was therefore moved 3.7 ml to the left for parameter estimation.

5. Parameter estimation—results and discussion

5.1. Estimation techniques

5.1.1. Method 1

The Langmuir MPM parameters $k_{ads0,i}/k_{des0,i}$ and β_i obtained from the linear gradient experiments were tuned in order to fit the simulated retention times for the different proteins to the experimental ones. This was done manually by changing β_i and $k_{ads0,i}/k_{des0,i}$ in an iterative process, using three different elution gradients.

5.1.2. Method 2

The equilibrium parameters in the SMA model ν_ι and $K_{eq,i}$ were adjusted to fit the peak position in the linear gradient experiments. At low concentration only ν_ι and $K_{eq,i}$ affect the peak position. The concentration of insulin was relatively high and to determine the linear parameters accurately the steric factor, σ_ι, must be correct. An iterative procedure between breakthrough experiments and retention maps must be implemented to determine the correct values for all three parameters in the SMA equilibrium expression. This iterative procedure is not necessary for transferrin and IgG.

The steric factor alone adjusts the position of the breakthrough curve if ν_ι and $K_{eq,i}$ are determined in earlier estimations. Only the breakthrough up to 97% is considered. Once the position has been accurately determined the apparent dispersion coefficient and kinetic parameter are varied to give the optimal least squares fit to the shape of the entire breakthrough curve for each pure component and concentration.

5.2. Void fraction

The void fraction in the RESOURCE 15 Q column is difficult to measure. The RESOURCE column contains monosized particles with very large pores. The large pores make it difficult to measure the column void with, for example, latex particles. Therefore, the column void was not measured experimentally. The column void fraction was set to 0.32 in the model based on previous experience. The void fraction is relatively low value, but this value is considered reasonable as the column was industrially packed.

5.3. Handling salt concentration in parameter estimation

The buffers used in the gradient elution experiments and in the breakthrough experiments have different conductivities. The conductivity and salt concentration of the sample and of the loading and elution buffers were measured. A linear relationship between salt concentration and conductivity is assumed. The tris (tris[hydroxymethyl]aminomethane) itself contributes with a conductivity of 0.1 mS/cm. Higher conductivity in the Tris–HCl is considered to be due to the interacting salt component. This assumption is considered reasonable considering that the desired pH in the buffers is achieved by adding HCl. The salt concentration in the buffers and samples was calculated from the conductivity.

5.4. Capacity and shape parameters in method 1

The maximum capacity, $q_{max,i}$ (mol/m^3 gel), was determined using the data file for the RESOURCE 15 Q, 1 ml column [26]. The supplier has determined the capacity, cap_{ref}, for BSA and lysozyme to be 50 and 100 mg/ml, respectively. Scaling the capacities with the molecular weights for IgG, transferrin and insulin, see Eq. (16), gives the value of q_{max} used in the simulations (see Table 2).

$$q_{max,i} = \frac{\text{cap}_{ref}(\text{Mw}_{ref}/\text{Mw}_i) \times 1000}{(1-\varepsilon_c)\text{Mw}_i} \tag{16}$$

The BSA reference capacity was used for IgG and transferrin and the lysozyme reference capacity for insulin. This is a rather good approximation as they have similar size and thus the same access to the pores in the beads.

Table 2
Molecular weights, maximum capacity and dispersion coefficients used for the estimation of the linear parameters for the different proteins included in this study

Protein	Mw (g/mol)	q_{max} (mol/m^3 gel)	D_{ax} (m^2/s)
IgG	150000	0.219	1.54×10^{-7}
Insulin	6000	57.2	1.54×10^{-7}
Transferrin	80000	0.770	1.54×10^{-7}
BSA	67000	1.10 [26]	–
Lysozyme	14000	10.5 [26]	–

Table 3
The inlet concentration in the experimental runs, estimated steric factor, desorption coefficient and apparent dispersion coefficient for the proteins used

Protein	IgG	Transferrin		Insulin	
Concentration (mg/ml)	–	2	4	5	18
k^*_{des} (mol/(m^3/s))	1.3×10^{-16}	2.0×10^{-8}	8.0×10^{-8}	8.0×10^{-8}	4.3×10^{-8}
σ	210	97	110	7.8	7.8
D_{ax} (m^2/s)	5×10^{-6}	4.4×10^{-6}	5.1×10^{-6}	4.5×10^{-6}	1.6×10^{-5}

The dispersion coefficient (see Table 2) was determined using an empirical correlation presented by Chung and Wen [27]:

$$Pe = \tfrac{1}{2}\varepsilon_c(0.2 + 0.011Re^{0.48}) \quad (17)$$

where the Peclet number and Reynolds number are defined as:

$$Pe = \frac{v_{int}d_p}{D_{ax}}, \qquad Re = \frac{v_{int}\rho\varepsilon_c d_p}{\eta} \quad (18)$$

where ρ is the density (kg/m^3) of the solution, d_p is the bead diameter (m), and η is the dynamic viscosity (Pa s) of the solution. The correlation by Chung and Wen gives a lower dispersion coefficient than that obtained from a breakthrough experiment, indicating that external mixing and the transport inside the bead are not included. In addition, the absolute value of $k_{des0,i}$ and $k_{ads0,i}$, with constant $k_{ads0,i}/k_{des0,i}$, was adjusted to give the elution peaks a reasonable peak width compared to the chromatograms in the linear gradient experiments, see Table 4

5.5. Capacity and shape parameters in method 2

5.5.1. Insulin and transferrin

The steric factor was determined by frontal chromatography with pure components and reasonable values were obtained [24,28], see Table 3. The amount of bound protein at different concentrations was used to determine a steric factor. The kinetic parameter, $k^*_{des,i}$, and the apparent dispersion coefficient, D_{ax}, were adjusted to fit the shape of the breakthrough curve for transferrin and insulin, see Figs. 2 and 3. With this method it is not necessary to use a very high protein concentration in the loading step to algebraically calculate the steric factor from q_{max}. The advantage of using a computer program to determine the steric factor is that a lower concentration, and therefore less protein, is needed for each experiment. The drawback of this method is the uncertainty in extrapolating the results from a lower concentration to a higher concentration.

The position and maximum value of the breakthrough is determined by the steric factor σ. The steric factor determines the equilibrium for the different proteins and should be approximately constant regardless of concentration of salt and protein for the same breakpoint. When extrapolating the results to the case of multi-component adsorption one drawback is that protein–protein interactions are not taken into account.

5.5.2. IgG

The monoclonal IgG that was studied in this work is not available on the open market. IgG with a sufficiently high concentration and in sufficient amounts to perform a meaningful breakthrough experiment could therefore not be obtained.

To obtain a crude estimate of the steric factor and the shape of the breakthrough curve, it was assumed that the steric factor is directly proportional to the molecular weight. Using this approach the steric factor for IgG was obtained using Eq. (19). The steric factor for IgG was calculated to be 210. This approach is considered to be reasonable as it works fairly well for transferrin and insulin. The steric factor is scalable between transferrin and insulin with reasonable accuracy as the steric hindering factor for transferrin should

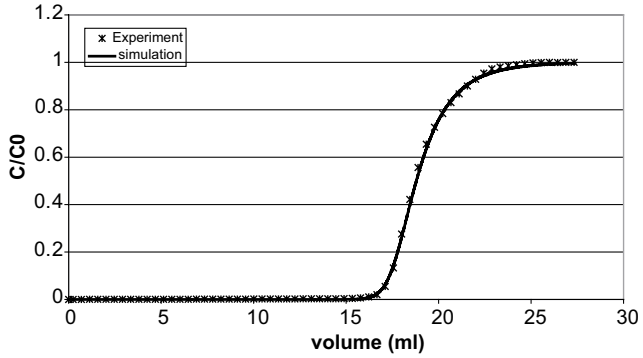

Fig. 2. Breakthrough curve for transferrin (2 mg/ml) used for estimation of the steric factor, desorption coefficient and apparent dispersion coefficient.

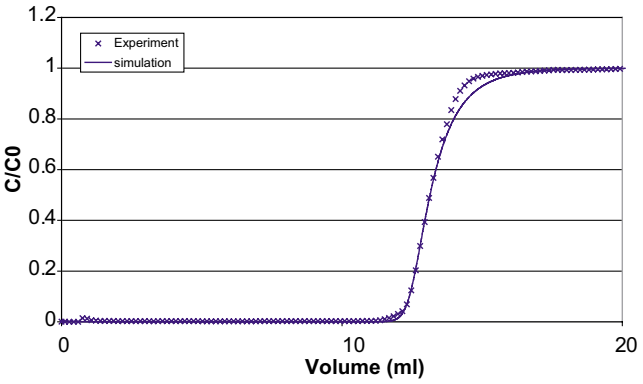

Fig. 3. Breakthrough curve for insulin (5 mg/ml) used for estimation of steric factor, desorption coefficient and apparent dispersion coefficient.

Table 4
The estimated linear parameters in the Langmuir MPM model

Protein	k_{ads0}/k_{des0}	k_{des0}	β
IgG	4.4×10^{-2}	0.250	4.4
Insulin	5.5×10^{-3}	5	2.9
Transferrin	2.5×10^{-3}	4000	3.0

be 116 according to this approach (see Table 3). The shape parameters $k^*_{des,i}$ and D_{ax} for IgG are set to give a reasonable shape of the breakthrough curve.

$$\sigma_{IgG} = \sigma_{insulin}\frac{150\,000}{5733} = 210 \quad (19)$$

5.6. Linear parameters, methods 1 and 2

5.6.1. Gradient elution

The gradient elution experiments were performed on an ÄKTA explorer 100 system with a large dead volume compared with the column volume. The retention times for the three components were corrected for the dead volume.

The ratio k_{ads0}/k_{des0} and the parameter β in the Langmuir MPM model and the parameters K_{eq} and ν in the SMA model were adjusted to find the correct peak position at different gradient slopes at pH 8.5. The various parameters determined for the three proteins for the Langmuir MPM model and the SMA model are reasonable [17,24,28] and given in Tables 4 and 5.

The estimated parameters for the elution step with a salt gradient of 60 column volumes are compared with the experimental results in Fig. 4. The second transferrin peak is that used for parameter estimation. As can be seen from the chromatograms the peak positions are estimated with relatively good accuracy for both models at 60 CV slope. The two small peaks after the insulin peak contain other proteins than the three in this study and were not used to evaluate the methods.

The gradient elution at 160 CV was used as a check and was not used for the determination of the linear parameters in the models. It can be seen from the validation experiment that the parameter estimation was good for IgG and insulin, see Fig. 5. The parameters for transferrin are more difficult to evaluate as the transferrin peak is split into three peaks and the content in each peak was not investigated.

5.6.2. Accuracy

The parameters for IgG, insulin and transferrin can determine the peak positions with relatively good accuracy. The

Table 5
The estimated linear parameters in the SMA model

Protein	K_{eq}	ν
IgG	0.50	6.8
Insulin	0.054	2.5
Transferrin	190	5.2

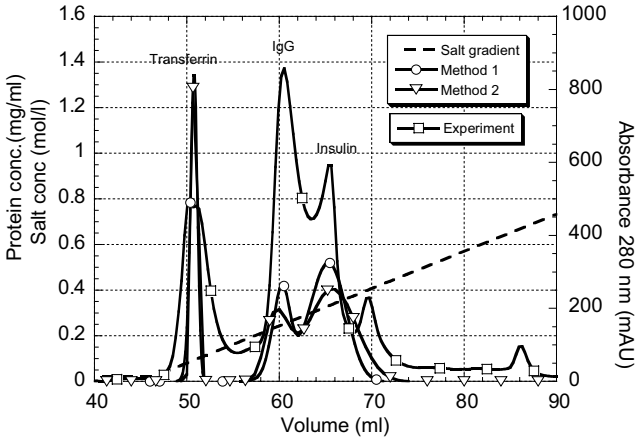

Fig. 4. Simulated, and experimental chromatogram for a gradient elution of 60 column volumes.

accuracy for transferrin is lower than for the other proteins. One possible explanation is that the transferrin peak contains a number of types of transferrin with slightly different p*I* values. This becomes evident at the shallowest gradient at pH 8.5, where the transferrin peak divides into a number of slightly differentiated peaks.

In method 1 the mean error on the peak position at three gradients (40, 60, 80 CV) used for parameter estimation is ±0.6% for IgG, ±0.3% for insulin and ±8.2% for transferrin. The overall error on the peak positions in method 2 at the three gradients (40, 60, 80 CV) used for parameter estimation is ±2% for IgG, ±0.6% for insulin and ±5% for transferrin. The lower accuracy for transferrin is probably due to the fact that the transferrin peak divides into two peaks at 60 and 80 CV.

The error in method 2 in the experiment with 160 CV is ±3.5% for IgG, and ±0.2% for insulin and. Method 1 gives an error of ±1.1% for IgG and ±1.5% for insulin at a gradient of 160 CV. The error for transferrin is difficult to evaluate as the peak divides into three different peaks.

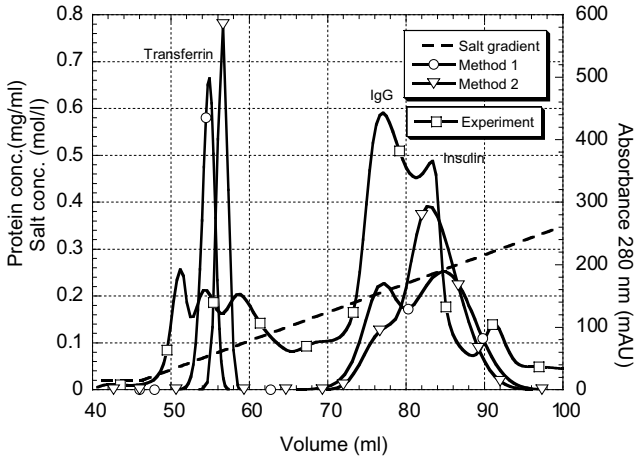

Fig. 5. Simulated, and experimental chromatogram for a gradient elution of 160 column volumes.

5.7. Comparison—models and methods

The difference between methods 1 and 2 lies in how the capacity and the shape of the peaks are obtained, i.e. steps 2 and 3 differ between the two methods in the general approach. Both models could be used in both methods. In this work methods 1 and 2 should be compared as a whole. An even more thorough method can be used to obtain more accurate predictions of the behavior of salt and protein in the column. Such a method should include mixing in the external volume of the experimental equipment and take into account the effects of protein–protein interaction, porosity and diffusion for salt and protein. That would most certainly be more successful in describing the system but would also require more experimental effort together with the additional work associated with modeling and parameter estimation. The choice of method is always a trade-off between accuracy and the amount work required.

The Langmuir MPM model could certainly be used in method 2 and would most probably give useful results. However, the approach in this work is to utilize an increased number of experiments to increase the physical significance of the model. Therefore the SMA model is used in method 2. Using the SMA model in method 1 proves to be more difficult. Using the estimated q_{max} in method 1, see Table 2, to calculate σ, see Eq. (20) [18], for the protein results in unreasonable steric factors.

$$q_{\max,i} = \frac{\Lambda}{\nu_i + \sigma_i} \tag{20}$$

To be able to correlate the steric factor it is believed necessary to know the linear SMA parameters for the proteins and to know at what conductivity the experimental breakthrough is obtained. If such information were available it would be possible calculate the steric factor for the protein investigated by the matrix producer and correlate the steric factor as shown in Eq. (19).

6. Validation of model predictability—results and discussion

One purpose of this work was to develop models that can be used in predicting the behavior of a mixture of proteins in an ion-exchange column. The predictability in multicomponent mixtures is of great importance when using models to predict breakthrough and separation in industrial solutions and when using the results for optimization and scale-up.

The validation experiment was performed with protein concentrations that were not used in the parameter estimation. The salt concentration in the loading step was also different from that used in the parameter estimation.

The validation was conducted as the normal separation procedure in ion-exchange chromatography at BioInvent International AB, i.e. the elution is conducted in two steps, where transferrin should be eluted in the first step and insulin and IgG in the second step.

The goals of the model application are:

1. to predict the position and composition of the breakthrough;
2. to predict the composition of the first elution peak; and
3. to predict the composition of the second elution peak and, in which order the components elute.

6.1. Validation experiment

The system used in the validation experiment was the ÄKTA Purifier-100 system. A mixture of insulin, transferrin, and IgG was loaded onto a column. The experiment was performed at a flow rate of 1 ml/min on a RESOURCE 15 Q column and the sample was loaded onto the column with a superloop. The concentrations of the proteins were determined using UV light at 280 nm and the salt concentration was measured with a conductivity meter. Fractions were collected during the entire experiment and were analyzed by gel filtration to determine the presence of the different components.

The conditions for the different steps are described as follows.

- Loading: a mixture of 0.30 mg/ml insulin, 0.91 mg/ml transferrin and 0.33 mg/ml IgG was loaded onto the column. The conductivity of the loading buffer was 3.2 mS/cm, which corresponds to 0.039 M NaCl. A 48 ml sample was loaded onto the column and fractions of the breakthrough were collected. The conductivity of the equilibration buffer was 1.3 mS/cm, which corresponds to 0.015 M NaCl.
- Washing: the conductivity of the buffer used for washing was 1.3 mS/cm, which corresponds to 0.015 M NaCl. The washing volume was 10 ml and 1 ml fractions were collected.
- Elution step 1: the conductivity in the first elution step was 5.4 mS/cm, which corresponds to a concentration of 0.067 M NaCl. The elution volume was 20 ml and 1 ml fractions were collected. Elution was achieved by mixing 1.015 M NaCl buffer with the original equilibration buffer.
- Elution step 2: the conductivity in the second elution step was 32 mS/cm, which corresponds to a concentration of 0.396 M NaCl. The elution volume was 20 and 1 ml fractions were collected. Elution was achieved by mixing 1.015 M NaCl buffer with the original equilibration buffer.
- The final elution was performed by loading of pure buffer solution of 82 mS/cm, 1.015 M NaCl, onto the column.

6.2. Results and discussion

The main goal of this study as mentioned above was to predict the position and shape of the breakthrough curve and to determine which protein elutes at a certain salt concentration. The results from method 2 was used in the

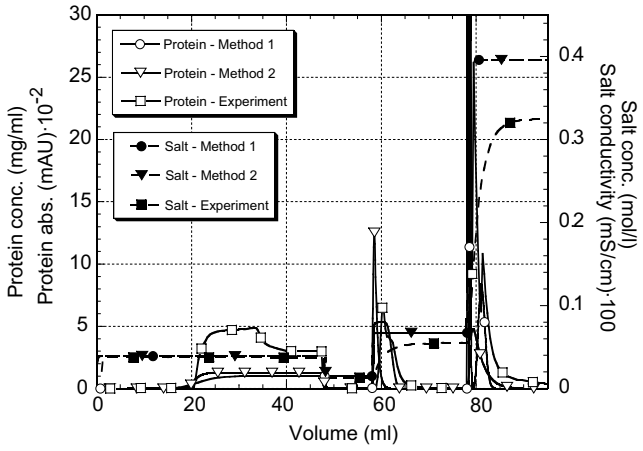

Fig. 6. The entire validation experiment including loading, washing, elutions 1 and 2. The experimental protein concentration is expressed as mAU $\times$ 10^{-2} and was determined UV light at 280 nm. The experimental salt gradient is expressed as mS/cm $\times$ 10^{2}.

experimental design of the validation experiment to determine suitable loading volume and conductivity in the sample as well as suitable conductivities in the two elution steps. Both methods are successful in predicting the overall behavior in the loading and separation steps. The entire cycle is shown for the simulation and the experimental run in Fig. 6.

6.2.1. Loading step

Simulated and experimental data for the loading step are shown in Fig. 7. The position for the mean volume for the breakthrough is in good agreement for both methods 1 and 2 compared with the experimental results, see Table 6. The 10% breakthrough prediction of both models is less accurate, see Table 6. Method 1 predicts breakthrough 3.4 ml earlier and method 2 1.3 ml earlier than the experimental breakthrough.

The shape of the breakthrough curve simulated according to method 2 is fairly correct whereas the breakthrough simulated according to method 1 is less steep. One explanation in this method is that a correlation is used for the dispersion coefficient and that the kinetic parameters are adjusted to give a reasonable peak width from the ÄKTA Explorer, which has a much larger dead volume than the ÄKTA Purifier. A larger dead volume results in a lower resolution and could partly explain the shallow breakthrough provided by method 1. The dip in the experimental breakthrough curve is probably due to protein–protein interactions in adsorption and these phenomenon are not considered in neither of the methods.

Table 6
The loaded volume at 10 and 50% breakthrough of the maximum concentration

	10% breakthrough (ml)	50% breakthrough (ml)
Experiment	20.8	21.5
Method 1	17.4	21.4
Method 2	19.5	20.8

6.2.2. Elution step 1

Simulations and experimental data for elution step 1 are shown in Fig. 8. The experiment was designed to elute only transferrin in this first elution step. The methods predict that only transferrin is eluted at this moderate salt concentration of 0.067 M NaCl. This was also observed in the experimental case as the gel filtration analysis shows that only transferrin is eluted. The shape of the elution peak is not accurately foreseen by the methods. This is partly due to the fact that that the experiment did not result in a perfect salt step in the elution and therefore gave rise to a steep salt gradient rather than a perfect step elution. Transferrin is also shown to divide into several peaks in the shallower gradient elution experiment used to check the linear parameters in both models. Generally, the peaks predicted by the methods elutes faster than the experimental ones, due to the shape of the elution step achieved by the ÄKTA Purifier. Another explanation of the difference between the peaks may be the

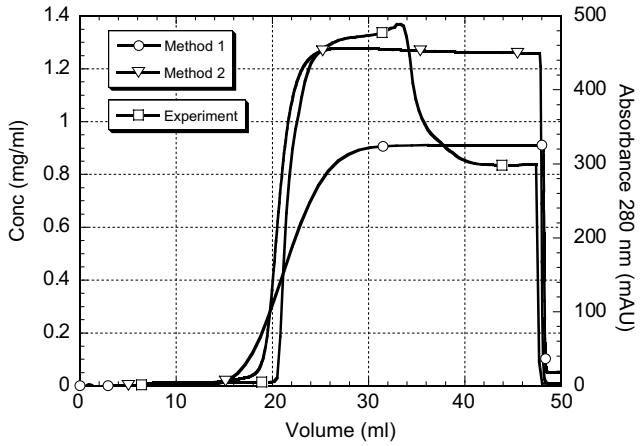

Fig. 7. The loading step showing predicted and experimental transferrin breakthrough.

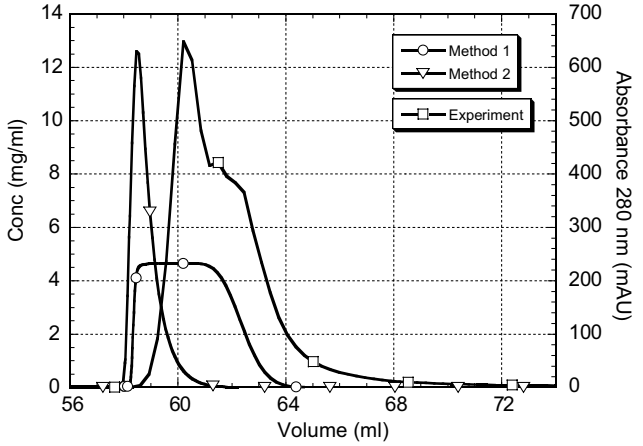

Fig. 8. Elution step 1 showing simulated and experimental elution of the transferrin peak.

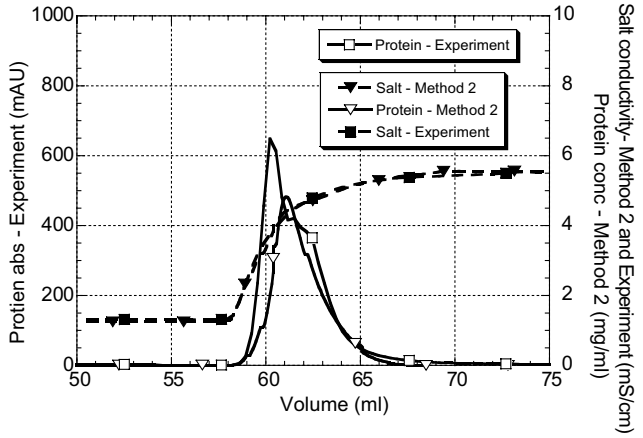

Fig. 9. Elution step 1 showing simulated and experimental elution of the transferrin peak with adjusted salt step.

dead volume between the mixing chamber and the column to which the elution buffer is applied. If the dead volume and shape of the salt step is considered the simulated peaks shift to a longer retention time as exemplified for elution step 1 and method 2 in Fig. 9.

6.2.3. Elution step 2

Simulations and experimental data for elution step 2 are shown in Fig. 10. The methods predict that IgG and insulin should be eluted in the second elution step, and that IgG will be eluted slightly before insulin. According to the models, transferrin has been completely removed in the first elution step. The validation experiment with a salt concentration of 0.4 M NaCl shows that the first elution step was not sufficiently long a small amount of transferrin was eluted at the beginning of the second elution step. The second and third peaks in the second elution step are IgG and insulin, which, in agreement with the method predictions are completely eluted. The gel filtration analysis clearly shows that the first peak is transferrin, the second IgG and the third insulin. Neither the shape nor the position of the elution peaks is accurately described by the methods, partly due to inaccuracies in the mathematical models and in the determination of the model parameters. Another explanation could be, as mentioned above, that elution is not performed as a perfect step in the experiment. The simulated peak position is generally earlier than the experimental, as was the case in elution step 1.

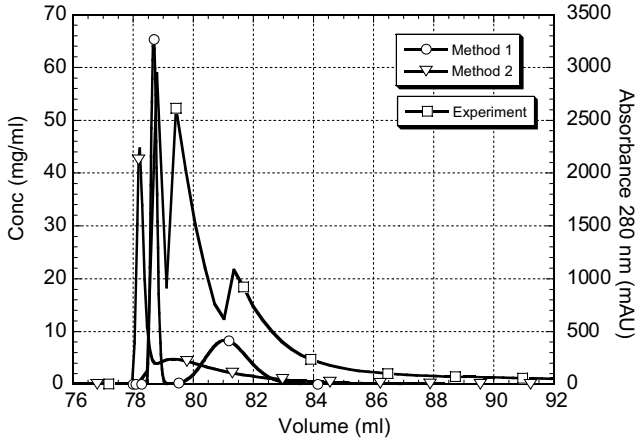

Fig. 10. Elution step 2 showing with simulated elution peaks of IgG followed by insulin. The experimental data show a peak of transferrin followed by IgG and insulin peaks.

7. Conclusions

The methods give calibrated models that succeed in predicting the separation of three proteins: IgG, transferrin and insulin, and can, with reasonable accuracy, predict the breakthrough of transferrin in a mixture of insulin, IgG and transferrin. It is thus reasonable to assume that the models can be used to investigate effects of different salt and protein concentrations. This is advantageous when designing a separation process as the effects of numerous combinations of process parameters can be investigated in advance by computer simulation and the experimental work can be reduced to investigating the optimal conditions according to the model.

This work shows that the normal experimental work, with some additional experiments, can be used for parameter estimation in adsorption equilibrium models. Both methods studied give calibrated models that have sufficient accuracy to be useful in process development. Method 2 gives a model with slightly more reliable results. The preferred method depends largely on the availability of pure components and the need for accurate results.

The methods suggested in this work include retention maps for optimal pH, gradient elution experiments, breakthrough curves and empirical correlations and has been proven to be an efficient approach in process development. Some additional experiments have to be performed to obtain the parameters in the models. The predictability achieved results in less experimental work in process design as a whole as the correct salt gradient/step and loading volume is screened experimentally today. These methods give models that can assist experimental design in the validation and in the development of an ion-exchange step in downstream processing. They can also provide a platform for modeling scale-up and optimization of protein purification processes.

8. Nomenclature

c_i	concentration of component i in the mobile phase (mol/m^3)
$c_{\text{inlet},i}$	inlet concentration of component i in the mobile phase (mol/m^3)
c_s	concentration of salt in mobile phase (mol/m^3)
cap_{ref}	column capacity of reference component (kg/m^3)
d_p	bead diameter (m)
D_{ax}	apparent dispersion coefficient (m^2/s)
$k_{\text{ads}0,i}$	modulator constant (m^3/mol s)

$k_{ads,i}$	adsorption coefficient, Langmuir MPM (m^3/mol s)
$k_{des0,i}$	modulator constant (m^3/mol s)
$k_{des,i}$	desorption coefficient, Langmuir MPM (1/s)
$k^*_{ads,i}$	adsorption coefficient, SMA (mol/(m^3/s))
$k^*_{des,i}$	desorption coefficient, SMA (mol/(m^3/s))
$K_{eq,i}$	equilibrium constant, SMA
K_i	equilibrium constant for component i, Langmuir MPM (m^3/mol)
L	length of the column (m)
Mw_i	molecular weight of component i (kg/mol)
Mw_{ref}	molecular weight of reference component (kg/mol)
q_i	concentration in the stationary phase for component i (mol/m^3 gel)
$q_{max,i}$	max concentration in the stationary phase for component i (mol/m^3 gel)
q_s	total concentration of salt ligands in the gel (mol/m^3)
$\bar{q}_s$	concentration of available salt ligands in stationary phase (mol/m^3)
$\hat{q}_s$	concentration of shielded ligands (mol/m^3)
r_i	reaction rate for protein i (mol/(m^3/s))
S	concentration of the elution component (mol/m^3)
t	time (s)
v_{int}	interstitial velocity (m/s)
x	axial coordinate along the column (m)

Greek letters

β_i	constant describing the IEC characteristic
ε_c	void fraction in the column (m^3 mobile phase/m^3 column)
γ_i	constant describing the HIC characteristic (m^3/mol)
η	dynamic viscosity (Pa s)
Λ	total concentration of binding sites in the gel (mol/m^3 gel)
ν_i	number of interacting sites between component i and gel
ρ	density (kg/m^3)
σ_i	steric factor

Acknowledgements

The Swedish Center for BioSeparation is gratefully acknowledged for financial support. BioInvent International AB, Lund, Sweden, is also acknowledged for materials and experimental support.

References

[1] H.I. Miller, Nat. Rev. Drug Discovery 1 (2002) 1007.
[2] G. Walsh, Eur. J. Pharm. Biopharm. 55 (2003) 3.
[3] E. Stoger, M. Sack, R. Fischer, P. Christou, Curr. Opin. Biotechnol. 13 (2002) 161.
[4] D.P. Pollock, J.P. Kutzko, E. Birck-Wilson, J.L. Williams, Y. Echelard, H.M. Meade, J. Immunol. Methods 231 (1999) 147.
[5] H.E. Chadd, S.M. Chamow, Curr. Opin. Biotechnol. 12 (2001) 188.
[6] H. Graf, J.-N. Rabaud, J.-M. Egly, J. Immunol. Methods 139 (1991) 135.
[7] B. Hunt, C. Goddard, A.P.J. Middelberg, B.K. O'Neill, Biochem. Eng. J. (2001) 135.
[8] N. Ameskamp, C. Priesner, J. Lehmann, D. Lütkmeyer, Bioseparation 8 (1999) 169.
[9] K. Huse, H.-J. Böhme, G.H. Scholz, J. Biochem. Biophys. Methods 51 (2002) 217.
[10] S. Oscarsson, D. Angulo-Tatis, G. Chaga, J. Porath, J. Chromatogr. A 689 (1995) 3.
[11] G. Iberer, H. Schwinn, D. Josic, A. Jungbauer, A. Buchacher, J. Chromatogr. A 921 (2001) 15.
[12] R. van Reis, A. Zydney, Curr. Opin. Biotechnol. 12 (2001) 208.
[13] E.L.V. Harris, in: S. Roe (Ed.), Protein Purification Techniques, Oxford University Press, Oxford, 2001, Chapter 6, p. 111.
[14] R.K. Scopes, Protein Purification—Principles and Practice, Springer-Verlag, Berlin, 1994, Chapter 6, p. 146.
[15] Amersham Biosciences, Antibody Purification—Handbook, Amersham Biosciences AB, Björkgatan 30, SE-751 84 Uppsala, Sweden, 2002.
[16] Amersham Pharmacia Biotech, Ion-Exchange Chromatography—Principles and Methods, Amersham Pharmacia Biotech, Björkgatan 30, SE-751 84 Uppsala, Sweden, 1999.
[17] W.R. Melander, S. El Rassi, Cs. Horváth, J. Chromatogr. 469 (1989) 3.
[18] C.A. Brooks, S.M. Cramer, AIChE J. 38 (1992) 1969.
[19] F. Carlsson, Mathematical modelling and simulation of fixed-bed chromatographic processes, Lund University, Lund, Sweden, Chem. Eng. 1 (1994) 1.
[20] T. Gu, Mathematical Modeling and Scale-up of Liquid Chromatography, Springer-Verlag, Berlin, 1995, Chapter 9, p. 95.
[21] The MathWorks Inc., MATLAB—the language of technical computing, The MathWorks Inc., 3 Apple Hill Drive, Natick, MA 01760-2098, USA, 2000.
[22] Process Systems Enterprise Ltd., gPROMS advanced user guide, Process Systems Enterprise Ltd., Bridge Studios, 107a Hammersmith Bridge Road, London W6 9DA, UK, 2001.
[23] E.S. Parente, B. Wetlaufer, J. Chromatogr. 355 (1986) 29.
[24] V. Natarajan, W. Bequette, S.M. Cramer, J. Chromatogr. A 876 (2000) 51.
[25] S.R. Gallant, S. Vunnum, S.M. Cramer, J. Chromatogr. A 725 (1996) 295.
[26] Amersham Biosciences, Source 15IEX, 18-1123-65, Data file, Amersham Biosciences AB, Björkgatan 30, SE-751 84 Uppsala, Sweden, 2002, pp. 1–8.
[27] S.F. Chung, C.Y. Wen, AIChE J. 14 (1968) 857.
[28] H. Iyer, S. Tapper, P. Lester, B. Wolk, R. van Reis, J. Chromatogr. A 832 (1999) 1.